Received: 9 November 2018 | Accepted: 6 December 2018

DOI: 10.1002/jcb.28369

RESEARCH ARTICLE

WILEY Journal of Cellular Biochemistry

Acetylcholinesterase with mesoporous silica: Covalent immobilization, physiochemical characterization, and its application in food for pesticide detection

Jeyanthi Palanivelu | **Ramalingam Chidambaram**

Department of Industrial Biotechnology, School of Bio-Sciences and Technology, Vellore Institute of Technology, Vellore, India

Correspondence
Ramalingam C, Department of Industrial Biotechnology, School of Bio-Sciences and Technology, Vellore Institute of Technology, Vellore 632014, Tamil Nadu, India.
Email: cramalingam@vit.ac.in

Funding information
Vellore Institute of Technology

Abstract

Toxic contamination of commonly consumed food products and water due to food chain vulnerability via agricultural products and commodities is a serious health hazard. This study reports on Santa Barbara Amorphous (SBA-15), a type of mesoporous silica nanoparticles, for efficient and stable acetylcholinesterase (AChE) adhesion toward detection of toxic pesticides. AChE was immobilized to the inert framework of mesoporous materials viz. SBA-15 with a proficient hydrolytic response toward acetylthiocholine. The immobilized system acts as a biosensor for the detection of pesticides, which are organophosphorus compounds in food. Both the SBA-15 and immobilized SBA-15 were characterized to give an insight on the physiochemical and morphological modification properties. The enzyme activity was accessed by Ellman's spectrophotometric bioassay for bare and enzyme-immobilized SBA-15 that resulted in promising enzymatic activity with the counterpart. Enzyme stability was also studied, which exhibited that immobilized AChE retained its catalytic activity up to 60 days and retained 80% of the hydrolytic activity even at 37°C. On the basis of the success of immobilized enzyme (covalent) being inhibited by acetylthiocholine, the sensor was administered for the inhibition by monocrotophos and dimethoate that are used widely as pesticides in agricultural. The inhibitory concentration (IC_{50}) value was found to be 2.5 ppb for monocrotophos and 1.5 ppb for dimethoate inhibiting immobilized AChE. This was verified using cyclic voltammetry, an electrochemical analysis thus proving that the SBA-15@AChE complex could be used as a sensitive and highly stable sensor for detecting the concentration of hazardous pesticide compounds.

KEYWORDS

acetylcholinesterase, acetylthiocholine, covalent immobilization, enzyme stability, inhibitory concentration 50, pesticides, Santa Barbara Amorphous

1 | INTRODUCTION

Pesticides are nondegradable chemical compounds that are widely used in the agricultural sector to prevent the proliferation of pest to achieve a good yield. Usually, the pesticides are supposed to be applied as a targeted deterrent for the pest. Yet, inadvertent infusion of these compounds into the product is difficult to avoid in the process.[1] If that happens and the product gets consumed without processing, it leads to several complications in humans, such as asthma, irritation, immunosuppression, endocrine disruption, inflammation, or combination of

these.[2-5] The usage of pesticides is common in modern agriculture as they are easy to synthesize, are low in cost, and destroy pests. All these factors indirectly contribute to high yield.[6] Mixtures of pesticides drift from the point of application to various systems like water, air, soil, and food in large amounts and get accumulated.[7] Toxic substances control act enabled in the United States of America 1976, categorized some pesticides that when accumulated were carcinogenic, mutagenic, and caused morphological changes in human erythrocytes.[8-10]

Acetylcholinesterase (AChE) is a key enzyme for the proper functioning of the central nervous system in both humans and insects. Pesticides that are a neurotoxin, by any means entering into the biological system will irreversibly inhibit AChE. They, in turn, contribute to the abnormal functioning of the vital organs leading to major problems due to the accumulation of neurotransmitter acetylcholine in nerves.[11-13] Consequently, pesticide residues at their lowest concentrations in food should also be detected owing to their toxicity and risk to human health.

AChE is widely studied and used as biosensing enzyme owing to its selectivity, sensitivity, and quick response by converting the enzymatic reaction into signal amplification in terms of electrochemical response or quantitative measurement of the enzyme activity through spectrophotometer analysis.[14] The molecular mechanism of pesticide inhibiting AChE is given in Figure 1.

As the analyte (pesticides) reacts with the bioreceptor (AChE), they produce biochemical signals. The intensity of the generated signals is directly proportional to the analyte concentration. The intensity can be observed as light signals in a spectrophotometric method commonly called as the Ellman's method or by using an electrochemical method using cyclic voltammetry. In this paper, the quality of the biosensor is validated using Ellman's methods and the results were verified using electrochemical method[15-17] via cyclic voltammetry.

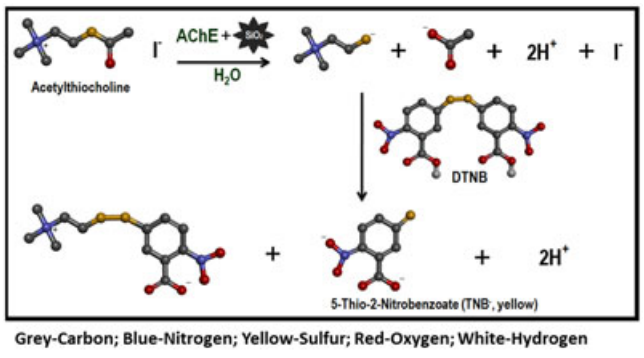

FIGURE 1 Molecular mechanism of AChE inhibition by pesticides. AChE, acetylcholinesterase; DTNB, 5, 5′-dithiobis-(2-nitrobenzoic acid)

A major concern in constructing biosensor is the immobilization material for the bioreceptor. The choice of the immobilization method on nanoparticles is an essential parameter that contributes for biosensor performances, largely in terms of stability, sensitivity, and selectivity by governing enzyme orientation, stability, mobility, structure, and biological activity.[18-20] In this study, we focused on ordered mesoporous material Santa Barbara Amorphous (SBA-15), which is an inorganic material having uniform pore channels with a size ranging from 2 to 50 nm. This makes them highly compatible host for bioactive substances enhancing catalysis, adsorption, separation, and also serves as a good nano reactor for molecular interactions to develop biosensors.[21-24] There are studies on many other mesoporous materials like zirconia-based electrochemical sensors[25] but mesoporous silica proved to be the best carrier when combined with enzyme for selective detection.[26-28]

Mesoporous silica holds properties like temperature-controlled enzyme release, delivery process, and intracellular monitored release and is also capable of detecting chromo fluorogenic sulfite ions in water.[29-33] Silica mesoporous as support capped with specific probes for sensing can detect different forms of anions, cations, various small molecules, and biomolecules.[34-36] In this regard, here, we aimed at capping AChE onto the synthesized SBA-15, and further characterization was done for making a stable biorecognition part of a biosensor. The main concern is to develop a sensitive and highly stable biorecognition complex of the biosensor, which was tested for its limit of detection of pesticides in soft drinks by Ellman's method and verified using cyclic voltammetry.

2 | MATERIALS AND METHODS

2.1 | Chemicals

Tetraethyl orthosilicate (TEOS), AChE (from *Electrophorus electricus*), acetylthiocholine (ATC), Tris (hydroxymethyl) aminomethane (Tris buffer), and 3-aminopropyl triethoxysilane (APTES) (99%) were purchased from Sigma-Aldrich (Bangalore, India). Hydrogen peroxide (30%), sulfuric acid (98%), methanol (99%), and ethanol (99.9%) were obtained from HiMedia Laboratories Pvt Ltd (Mumbai, India). Analytical grade monocrotophos was purchased from Sigma-Aldrich. All reagents supplied were of analytical grade and were used without further purification. Throughout the procedures, double deionizer (DI) water was used. The stock solution of monocrotophos and dimethoate (10^{-3} M) were prepared freshly in ethanol and further, the solutions were diluted with deionized water (Milli-Q, Pall

Corporation - Cascada™ LS-water Purification System) to an appropriate dilution for further experimental use. AChE (0.10 UML^{-1}) and ATC (100 mM) stock solutions were prepared using phosphate-buffered saline (PBS) (10 mM, pH 7.4) and stored in the refrigerator at 4°C when not in use.

2.2 | Synthesis of mesoporous silica nanoparticles SBA-15

SBA-15 was synthesized[37] using Pluronic P123 (EO_{20}-$PO_{70}EO_{20}$) polymer (3 g), which was dissolved in 80 mL of 2M HCl and 20 mL of H_2O by continuous stirring. 8.8 mL of TEOS was added dropwise. The solution mixture was stirred at room temperature (RT) (40°C) for 20 hours and then kept for 48 hours at 110°C. The mixture was cooled to RT and the solid was recovered by filtration followed by washing it with deionized water and air dried. As a final step to obtain pure SBA-15, the powder was calcinated at 550°C for 5 hours to remove the residual template materials (Supporting Information Figure S1).

2.3 | Immobilization of AChE enzyme onto mesoporous SBA-15 nanoparticles

The process used in this study was amino silanization of SBA-15, which was followed by enzyme attachment using the linker glutaraldehyde. This bonding makes the enzyme stable on the carrier without affecting the enzyme activity.[38] Ten milligrams per milliliter of SBA-15 was refluxed with APTES in the presence of dry toluene (110°C, 24 hours); pH was maintained at 8. After which the dichloromethane was washed and vacuum dried and stored at 4°C until further use. This product was stirred with 1 mg/mL of AChE in 0.1 mol/L phosphate buffer for 30 minutes at pH 8. The resultant product was then centrifuged to remove the unbound enzyme. The product was mixed with 1.5 mmol/L of glutaraldehyde (37°C, 1 hour) completing covalent immobilization of AChE in SBA-15. AChE-APTS/glutaraldehyde functionalized SBA-15 was stored in PBS at 4°C overnight (Supporting Information Figure S2). The efficiency of the enzyme activity was spectrophotometrically confirmed, which gives the immobilization competence. The complex was stored at 4°C until further use.

2.4 | Characterization

Confirmatory characterization was performed by employing the following methods.

- X-ray diffractograms (XRD) of SBA-15 and AChE@SBA-15 were dropped cast on an amine functionalized glass surface, followed by drying in vacuum overnight. The samples were scanned over a range of 20° to 90°.
- Fourier-transform infrared spectrometer (FTIR) analysis to obtain spectra of functional groups between the ranges of wavenumber 500 to 4000 cm^{-1}.
- The morphology of the prepared material was observed using scanning electron microscopy (SEM).
- The high resolution—transmission electron microscope (HR-TEM) was used to look at the porous structures of SBA-15.
- Nitrogen sorption studies (Brunauer, Emmett and Teller [BET]): SBA-15 was subjected for prediction of surface area with micromeritics between the relative pressure ranges from 0.0 to 1.0. Approximately, 0.036 g of SBA-15 sample was degassed at 450°C for a period of 12 hours. Outgassing was done for 1 hour at 100°C before the analysis. Nitrogen gas was used for analysis.
- The isotherm curve exhibiting the pore size distribution is obtained as a result of performing desorption analysis by Barrett-Joyner-Halenda (BJH).

Details on instrumentations and methods are given in the Supporting Information File.

2.5 | AChE@SBA-15 complex inhibition studies on ATC

To check the hydrolyzing efficiency of the enzyme AChE immobilized on the mesoporous material SBA-15, enzymatic activity was performed for AChE and SBA-15-embedded AChE separately. Ellman's reagent was prepared using 0.032 g of 5,5′-dithiobis-(2-nitrobenzoic acid) (DTNB) in 0.1M phosphate buffer (pH 7.4). Ten microliters of bare enzyme and mesoporous silica containing enzyme were added to the wells of a 96-well microtiter plate. Varying volumes of ATC (10-250 ppm) was added to the wells and was incubated for 20 minutes. Spectrophotometric readings were taken at 412 nm immediately and after 20 minutes in a microplate reader (Lark-mr960; wavelength range 405-630 nm). The degree of inhibition was calculated according to Equation (1)

$$I\% = \frac{(A_i - A_0)}{A_i} \quad (1)$$

where $I\%$ is the percentage of inhibition, A_i is absorbance of a sample containing ATC, and A_0 is the absorbance in phosphate buffer.[39]

2.6 | AChE@SBA-15 complex inhibition studies on pesticides

The AChE immobilized on the mesoporous silica is used to inhibit pesticide. Different concentrations of the pesticide were prepared: monocrotophos and dimethoate

(100%, 50%, and 10%). The preprepared enzyme that immobilized SBA-15 was suspended in 5.5 mL of phosphate buffer (pH 7.4). Nine hundred microliters of immobilized enzyme was added to an Eppendorf tube to which 10 μL of the pesticide was added, along with acetylthiocholine. A hundred microliters of chromophore DTNB was added in the tube. Absorbance was measured 20 minutes after adding the DTNB at 412 nm. The degree of inhibition was calculated using Equation (1). The inhibition percentage obtained is directly proportional to the amount of pesticide.

2.7 | Electrochemical method for pesticide detection

Cyclic voltammetry was done for verifying the detection of monocrotophos and dimethoate using a CHI 440B (CH Instruments) workstation. It consists of a three-electrode cell using a glassy carbon electrode (GCE) as a working electrode (area 0.07 cm^2), saturated Ag/AgCl as a reference electrode and Pt wire as a counter electrode. For pretreatment of the modified electrode, silica immobilized with AChE was dispersed in ethanol and coated onto the GCE and was potentially cycled in ATC with window − 0.2 to +0.8 V for 10 cycles in a nitrogen purged at pH 7 of PBS. It is referred to as a control. For pesticide detection, in the same cell that has ATC, 2.5 μL of monocrotophos and 1.5 μL of dimethoate were added separately and 10 cycles performed with window −0.2 to +0.8 V (Northampton, MA). The data were interpreted using Origin software (version 8).[40,41]

2.8 | Stability of the enzyme fabricated on SBA-15

The storage stability of the enzyme fabricated on SBA-15 was checked by analyzing the enzymatic activity of AChE once every month till 6 months. The storage temperature stability was also investigated for the immobilized enzyme by maintaining it at 4°C, 25°C, and 37°C (RT) after which the enzyme activity was analyzed. Inhibition percentage of the substrate on the enzyme was calculated at the end, which is directly proportional to the stability of the enzyme. Zeta potential analysis was also done for immobilized SBA-15 at each time intervals. This was to check the stability of SBA-15 by dynamic light scattering. For instrumentation details, refer Supporting Information File.

2.9 | Determination of sensory effect in real-time samples

In any real-time sample, detection and accuracy of the fabricated sensor are measured through spike and recovery mode. Soft drink 1 and soft drink 2 were bought from the local supermarket, Vellore. The soft drinks were filtered through a 0.22-μm membrane. After which different concentrations of monocrotophos and dimethoate (10, 50, and 100 μg/L) were added in soft drinks to estimate the recovery percentage under optimum conditions.

2.10 | Statistical analysis

Experiments were statistically analyzed and expressed as the mean of parallel triplicates ($n = 3$) of one-way analysis of variance correlation in GraphPad Prism, version 5 software (San Diego, CA). $P < 0.05$ was considered as statistically significant.[15]

3 | RESULTS AND DISCUSSION

In this study, we have successfully synthesized mesoporous silica nanoparticles SBA-15. This form of mesoporous silica (SBA-15) has a high surface area to volume ratio making it an effective material for biomolecule immobilization. This report details the successful immobilization of AChE enzyme to mesoporous SBA-15 by the simple stirring process. Both the bare and enzyme-immobilized SBA-15 were subjected to various characterization techniques to validate the efficiency of the enzyme immobilization.

3.1 | X-ray diffractograms

Figure 2 shows the low-angle XRD patterns for SBA-15 and AChE-immobilized SBA-15, which displayed three well-characteristic intensive diffraction peaks (2θ) in the range 1.24° to 2.14°, indexed as (100) and (210) diffractions attributes toward the presence of highly ordered mesoporous silica-SBA-15 with a two-dimensional hexagonal symmetry (space group 6 pmm). This XRD pattern coincides to that of the previous characteristic studies made with specific mesoporous silica-SBA-15.[42] Besides, in the case of enzyme-immobilized SBA-15, the intensity of the diffraction peak $2\theta = 1.24°$ decreased and the other peaks were not noted. This phenomenon was due to the reduction in the pore volume and the percentage of the pores on SBA-15, which confirmed the immobilization of the enzyme.

3.2 | FTIR spectra of the SBA-15 silica nanoparticles

APTES functionalized SBA-15 and AChE immobilized on the functionalized SBA-15 are represented in Figure 3.

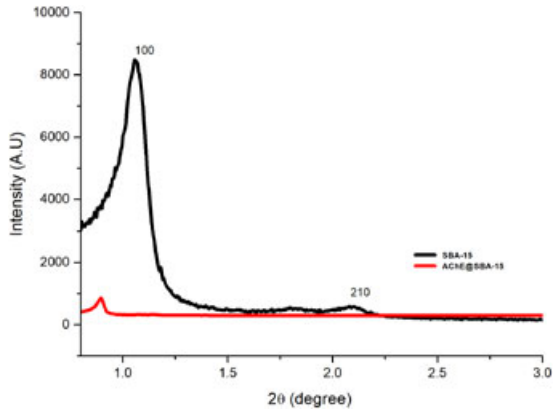

FIGURE 2 X-ray diffractograms spectra of SBA-15 and AChE-immobilized SBA-15. AChE, acetylcholinesterase; SBA-15, Santa Barbara Amorphous

SBA-15 IR spectra showed absorption characteristic peaks at Si–OH, Si–CH_2, Si–O–Si, Si–C, C–O, and O–H bonds. The band at 1067 cm^{-1} was due to the anti-symmetrical stretching vibrations of Si–O–Si. The bands at 797 cm^{-1} could correspond to the free silanol Si–OH stretching on the surface of the amorphous silica surface.[42] The band at 1725 cm^{-1} was due to Si–CH_2. As a result of APTES immobilization (APTES@SBA-15), a band was formed at 3412 cm^{-1} that corresponded to NH_2.

In IR spectra of AChE@SBA-15, the vibrations of bending bands were observed. Here, for the band at 1053 cm^{-1} (Si–O–Si) the stretching vibration length had decreased and the width had lessened and a new band at 1206 cm^{-1} was noticed when compared with the SBA-15 band at the same point. This could correspond to the enzyme immobilization effect on the surface of the APTES-functionalized porous mesoporous SBA-15 silica nanoparticles.[43]

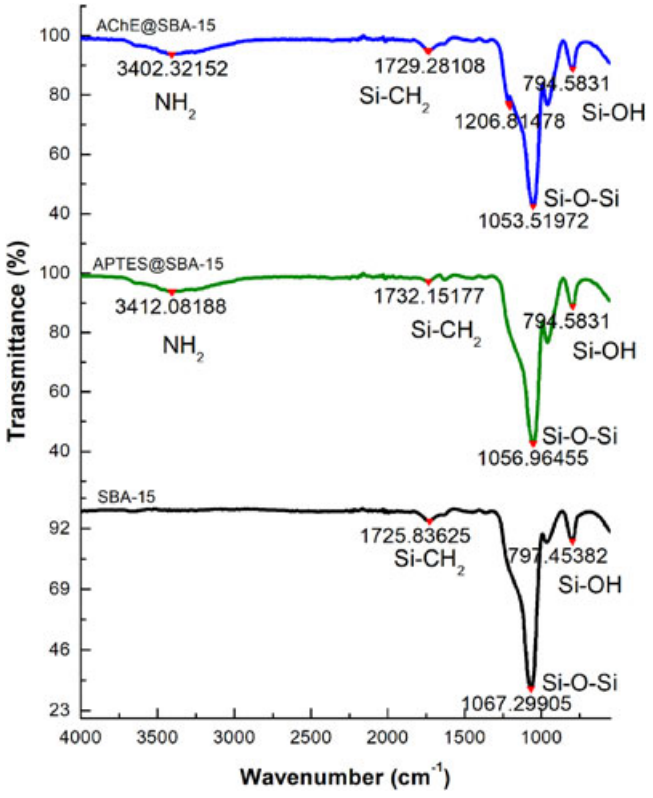

FIGURE 3 Fourier-transform infrared spectra of SBA-15 and AChE-immobilized SBA-15. AChE, acetylcholinesterase; APTES, 3-aminopropyl triethoxysilane; SBA-15, Santa Barbara Amorphous

3.3 | Scanning electron microscopy

Figure 4A and 4B, SEM results gave an insight into the morphological and aggregation pattern for SBA-15 and enzyme-immobilized SBA-15.[42] The image of the both SBA-15 and AChE-immobilized SBA-15 exhibited elongated tube-like structures with slightly increased aggregation in enzyme-immobilized SBA-15. This revealed that there was a slightly visible aggregation observed when the enzyme was immobilized to the mesoporous structure.[34,35]

3.4 | Transmission electron microscope

Figure 4C represents a TEM image of SBA-15 well evidenced the defined honeycomb-like hexagonal structures with uniform pore size at 200 nm magnification. The diameters of the pores were around 10.2 nm and the sizes of the particles were found to be 140 to 210 nm at

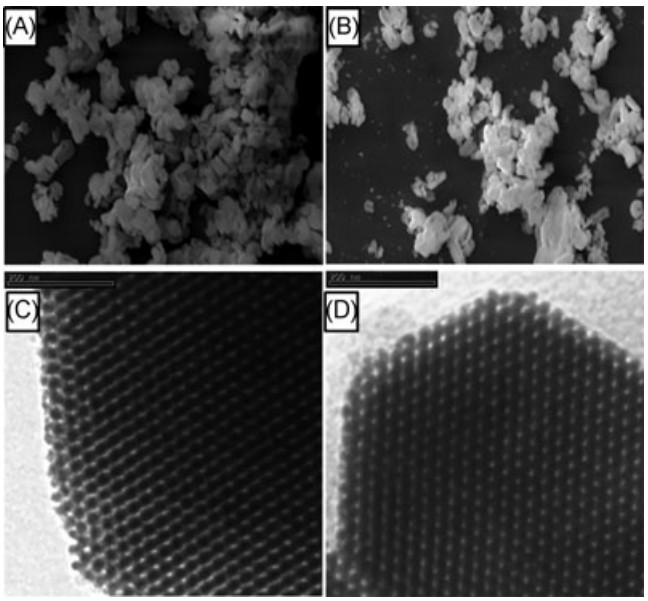

FIGURE 4 A, Scanning electron microscopy image of SBA-15; B, Scanning electron microscopy image of acteylcholinesterase-immobilized SBA-15; C, Transmission electron microscopy image of SBA-15; D, Transmission electron microscopy image of acteylcholinesterase-immobilized SBA-15

TABLE 1 Surface and porosity characterization of SBA-15 and enzyme-immobilized SBA-15

Samples	MSA, m^2/g	TSA, m^2/g	MSA/TSA	PD, nm	TPV, cc/g
SBA-15	392.759	538.494	0.72	4.099/40 Å	0.552
AChE@SBA-15	245.582	350.659	0.70	4.074/40 Å	0.393

Abbreviations: AChE, acetylcholinesterase; MSA, micropore surface area; MSA/TSA, a fraction of micropore surface area to the total BET surface area; PD, pore diameter; SBA-15, Santa Barbara Amorphous; TPV, total pore volume; TSA, total BET surface area.

1 μm magnification. The size range shows that it is highly compatible with AChE immobilization as the pore size is larger than the enzyme's molecular dimension. Figure 4D represents a TEM image of enzyme-immobilized SBA-15 where the pore diameter was reduced to 7.95 nm, which revealed the presence of the enzyme. The structure appears with uniform 2D hexagonal pores with the similar orientation as that of the SBA-15.[35,42]

3.5 | BET analysis

Physiochemical properties and textural properties of SBA-15 before and after ligand immobilization were analyzed by nitrogen sorption studies given in Supporting Information Figures S3 and S4, respectively. Physiochemical parameters like total pore volume, total surface area, and pore diameter for SBA-15 and AChE enzyme-immobilized SBA-15 are given in Table 1. The micropore surface area and the total BET surface area of SBA-15 were 392 and 538.49 m^2/g, respectively. Whereas, when SBA-15 was treated with a ligand, the micropore and total BET surface area was 245.5 and 350.6 m^2/g, which greatly reduced the proving of proper immobilization process.[42]

3.6 | Inhibition assay for the AChE biosensor

Figure 5A and 5B are plotted based on the concentrations of pesticides against the inhibition percentage of the enzyme AChE. Inhibition experiments were conducted in triplicates and analyzed using GraphPad Prism (pro 8) software (San Diego, CA). The calculated half-maximum inhibitory concentration (IC_{50}) value on the immobilized AChE by the selective pesticides monocrotophos and dimethoate were 2.5 and 1.5 ppb, respectively, which when compared with the earlier reports were based on an enzymatic method for pesticide detection (Table 2) and found to possess good detecting ability. The IC_{50} value represented the efficiency of a pesticide to act on AChE and to stops its action with the substrate. High IC_{50} level related to high inhibition level that corresponded to the toxic level of the pesticide.[47] In this case, both monocrotophos and dimethoate inhibited AChE, in which monocrotophos exhibited increased toxicity when compared with dimethoate.

3.7 | Storage stability

The fabricated complex showed good stability till 60 days with a decrease in the activity by 37%. After 30 days, bare AChE, when subjected to spectrophotometry bioassay resulted in the loss of its hydrolytic property below 50%, whereas immobilized AChE showed 82% of the enzyme activity as shown in Figure 6. The thermal stability of the bare and immobilized AChE was tested by maintaining them at different temperatures like 4°C, 25°C, and 37°C and subjecting them to spectrophotometry bioassay. This study resulted in proving the efficacy of the immobilization by increasing the stability, shelf life, and conventional use. The enzyme activity was maintained up to 80%, as shown in Figure 6, for immobilized AChE even at RT. It was evident from the result that the immobilized enzyme retained its enzyme activity at a higher level than that of the bare enzyme and was quite efficient than the previous report.[43,48] For better efficiency, the fabricated AChE@SBA-15 was stored at 4°C till usage.

Zeta potential was performed for SBA-15 on day 1 and day 40. The stability of SBA-15, in the beginning, was −44.5 mV, which is highly stable in nature (Supporting Information Figure S5A). A mild reduction was noted on

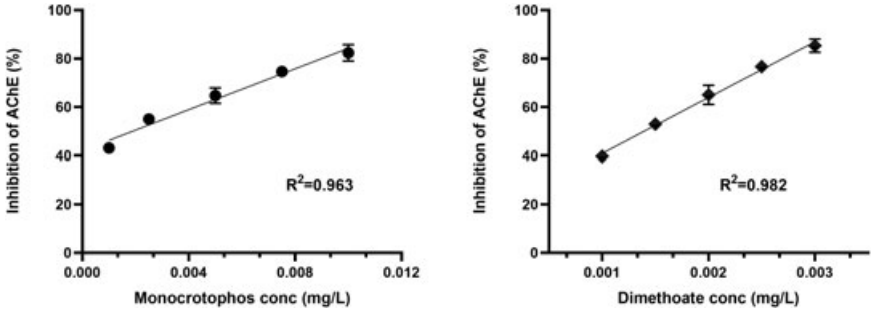

FIGURE 5 Inhibition effect of the pesticide on acetylcholinesterase (AChE)

TABLE 2 Assessing different nanoparticles for enzyme immobilization used in pesticide detection

Nanoparticles used in sensing	Detection methods	Pesticide detected	LOD	References
Silica thin film	Electrochemical	Paraquat	10 nM	[17]
Silver nanoparticles	Colorimetric	Malathion	0.455 nM	[44]
		Trichlorfon	5.46 nM	
Nickel	Electrochemical	Paraoxon	0.001 nM	[45]
Iron oxide	Amperometric	Malathion	0.1 nM	[46]
		Chlorpyrifos	0.1 nM	
		Monocrotophos	1 nM	
		Endosulfan	10 nM	
SBA-15 mesoporous particle	Spectrophotometer and electrochemical verification	Monocrotophos	2.510 ppb	Present work
		Dimethoate	1.5 ppb	

Dimethoate: an acaricide; monocrotophos: an organophosphate insecticide.

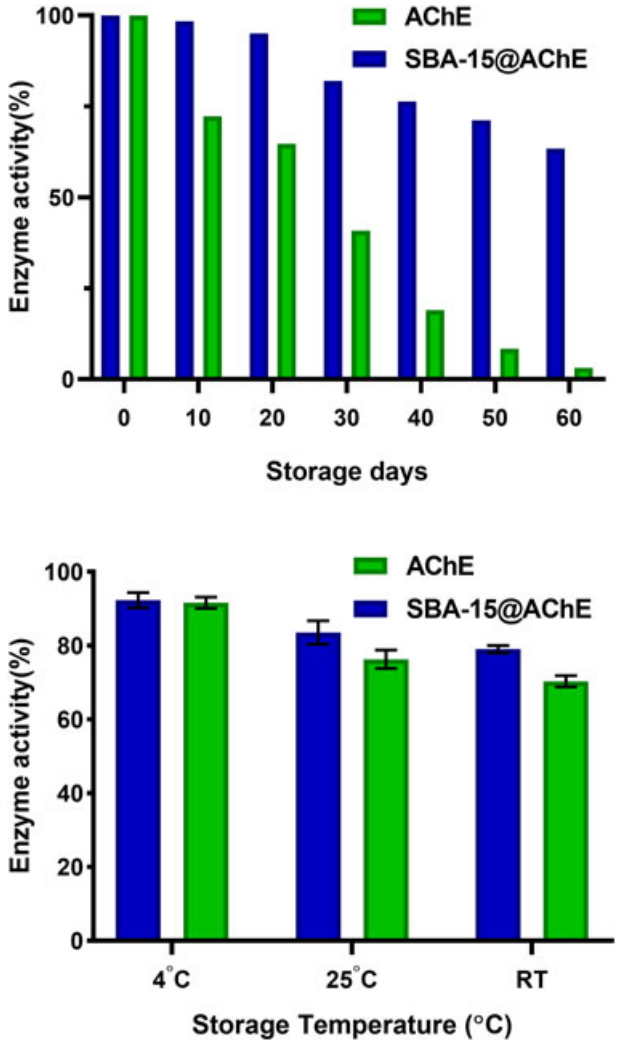

FIGURE 6 Storage stability of free AChE and SBA-15-immobilized AChE. AChE, acetylcholinesterase; SBA-15, Santa Barbara Amorphous

the 40th day exhibiting −40.7 mV, which is even more stable. This confirms the stability of SBA-15, making it more suitable for enzyme immobilization (Supporting Information Figure S5B).

3.8 | Electrochemical method detection

The cyclic voltammetric (CV) characteristics of thiocholine, which was produced due to the hydrolysis of AChE in the presence of ATC and pesticide, was studied using enzyme-immobilized silica-modified electrode in potential across −0.2 to 0.8 V in phosphate buffer, Figure 7(a) and (b). A bare GCE, AChE@silica-modified electrode in the absence of substrate ATC did not give any peak, which may be due to the absence of electron conduction.[26,28] In Figure 7(c), ATC was added in the substrate cell and the CV was characterized by oxidation

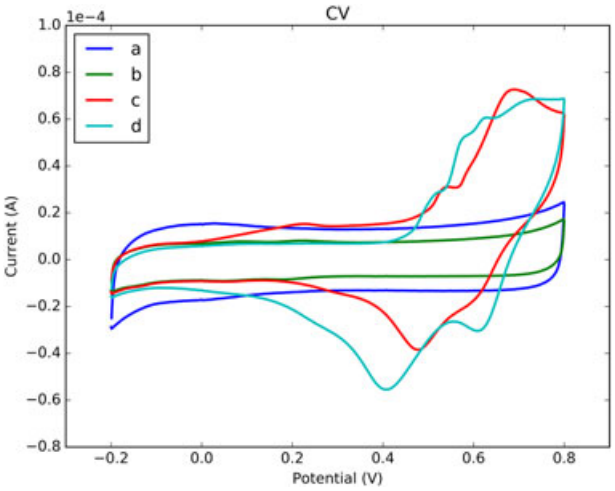

FIGURE 7 Cyclic voltammetry (CV) behavior of the fabricated biorecognition system

TABLE 3 Detection of pesticides in real-time samples

Pesticides	Spiked level, μg/L	Soft drink 1			Soft drink 2		
		Obtained, μg/L	Recovery, %	RSD, % ($n = 3$)	Obtained, μg/L	Recovery, %	RSD, % ($n = 3$)
Dimethoate	10	9.5	95	0.95	9	90	0.975
	50	47.2	94.4	0.42	44.3	88.6	0.57
	100	96.4	96.4	0.73	93	93	1.06
Monocrotophos	10	9.4	94	1.05	9.1	91	0.63
	50	43.2	86.4	1.19	42.7	85.4	0.85
	100	97.1	97.1	0.95	94.1	94.1	1.03

Abbreviation: RSD, relative standard deviation.

peak, which was detected due to the oxidation process of thiocholine by the enzyme. Whereas, in Figure 7(d), the pesticide was added in the same substrate cell along with the ATC, the oxidation peak reduced due to the pesticide inhibition of enzyme activity on ATC.[49]

3.9 | Real-time sample analysis

The sensory competence of the fabricated biorecognition system to quantify different concentrations of monocrotophos and dimethoate were analyzed by spiking the pesticides at different concentrations (10, 50, and 100 μg/L) in real samples like soft drink 1 and soft drink 2. Each known concentration samples were added to 1000 μL complex solution containing an immobilized enzyme, acetylthiocholine as substrate, and chromophore DTNB. The sample was left undisturbed for the enzyme activity to happen for 20 minutes, after which, the absorbance of each know concentration samples were measured with a spectrophotometer at the wavelength of 412 nm. The results were used to validate the potential of the system. Table 3 summarizes the results of recovery percentage and relative standard deviation value. The obtained results were found to be satisfactory in terms of good recovery in the real-time sample for detection of selected pesticides.

4 | CONCLUSION

This study proposed fabrication of stable enzymatic sensory complex for detecting pesticides. SBA-15 has large quantities of hydroxyl groups forming strong hydrogen bonds, which makes a platform for immobilizing AChE and prevent them from leaking out and are highly biocompatible. They also provide thermal stability for the enzyme. The adopted process helps in simple, highly reproducible, and quantitative analysis of different pesticides in food as pesticides are capable of attacking the hydrolysis process, henceforth reducing the AChE activity. This property of pesticides on AChE makes enzyme-based detection of pesticide an efficient process. Investigation of toxic pesticides like monocrotophos and dimethoate using this method in soft drinks showed the satisfactory limit of detection. The minimal detection level for monocrotophos and dimethoate were 2.5 and 1.5 ppb, respectively. The stability of the enzyme enhances higher response during the enzymatic hydrolysis reaction for accurate detection. This proposed method exhibits good accuracy on the delayed usage of the biosensor over a time period of 60 days and is thermally stable when compared with other biosensors. Following this quick, reliable, and simple method, cost-effective pesticide detection strips can be developed.

ACKNOWLEDGMENTS

This study was supported by Vellore Institute of Technology, Vellore, TN, India, by providing financial help for the project under the category of RGEMS-VC fund, VIT.

CONFLICTS OF INTEREST

The authors declare that there are no conflicts of interest.

AUTHOR CONTRIBUTIONS

Conceived and designed the experiments: RC. Performed the experiments, analyzed the data, and wrote the manuscript: JP. Revised manuscript critically for important intellectual content: RC.

REFERENCES

1. Bateman R. Rational pesticide use: spatially and temporally targeted application of specific products. *Optimising Pesticide Use*, 2003:131-159.
2. Fukuyama T, Tajima Y, Hayashi K, Ueda H, Kosaka T. Prior or coinstantaneous oral exposure to environmental immunosup-

pressive agents aggravates mite allergen-induced atopic dermatitis-like immunoreaction in NC/Nga mice. *Toxicology*. 2011;289(2-3):132-140.
3. Kjeldsen LS, Ghisari M, Bonefeld-Jørgensen EC. Currently used pesticides and their mixtures affect the function of sex hormone receptors and aromatase enzyme activity. *Toxicol Appl Pharmacol*. 2013;272(2):453-464.
4. Michielsen C, Zeamari S, Leusink-Muis A, Vos J, Bloksma N. The environmental pollutant hexachlorobenzene causes eosinophilic and granulomatous inflammation and in vitro airways hyperreactivity in the Brown Norway rat. *Arch Toxicol*. 2002;76(4):236-247.
5. Amaral AFS. Pesticides and asthma: challenges for epidemiology. *Front Public Health*. 2014;2:6.
6. Meng X, Wei J, Ren X, Ren J, Tang F. A simple and sensitive fluorescence biosensor for detection of organophosphorus pesticides using H_2O_2-sensitive quantum dots/bi-enzyme. *Biosens Bioelectron*. 2013;47:402-407.
7. Laetz CA, Baldwin DH, Collier TK, Hebert V, Stark JD, Scholz NL. The synergistic toxicity of pesticide mixtures: implications for risk assessment and the conservation of endangered Pacific salmon. *Environ Health Perspect*. 2008;117(3):348-353.
8. Monosson E. Chemical mixtures: considering the evolution of toxicology and chemical assessment. *Environ Health Perspect*. 2004;113(4):383-390.
9. Aragay G, Pino F, Merkoçi A. Nanomaterials for sensing and destroying pesticides. *Chem Rev*. 2012;112(10):5317-5338.
10. Suwalsky M, Rodríguez C, Villena F, Sotomayor CP. Human erythrocytes are affected by the organochloride insecticide chlordane. *Food Chem Toxicol*. 2005;43(5):647-654.
11. Piro B, Reisberg S. Recent advances in electrochemical immunosensors. *Sensors*. 2017;17(4):794.
12. Wen W, Yan X, Zhu C, Du D, Lin Y. Recent advances in electrochemical immunosensors. *Anal Chem*. 2016;89(1):138-156.
13. Zhang Q, Xu Q, Guo Y, Sun X, Wang X. Acetylcholinesterase biosensor based on the mesoporous carbon/ferroferric oxide modified electrode for detecting organophosphorus pesticides. *RSC Adv*. 2016;6(29):24698-24703.
14. Vimala V, Clarke S, Urvinder Kaur S. Pesticides detection using acetylcholinesterase nanobiosensor. *Biosens J*. 2016;5(133):2.
15. de Figueiredo-Filho LCS, Baccarin M, Janegitz BC, Fatibello-Filho O. A disposable and inexpensive bismuth film minisensor for a voltammetric determination of diquat and paraquat pesticides in natural water samples. *Sens Actuators B*. 2017;240:749-756.
16. Ellman GL, Courtney KD, Andres V, Jr, Featherstone RM. A new and rapid colorimetric determination of acetylcholinesterase activity. *Biochem Pharmacol*. 1961;7(2):88-95.
17. Nasir T, Herzog G, Hébrant M, Despas C, Liu L, Walcarius A. Mesoporous silica thin films for improved electrochemical detection of paraquat. *ACS Sens*. 2018;3(2):484-493.
18. Ghosh Chaudhuri R, Paria S. Core/shell nanoparticles: classes, properties, synthesis mechanisms, characterization, and applications. *Chem Rev*. 2011;112(4):2373-2433.
19. Liu G, Wang S, Liu J, Song D. An electrochemical immunosensor based on chemical assembly of vertically aligned carbon nanotubes on carbon substrates for direct detection of the pesticide endosulfan in environmental water. *Anal Chem*. 2012;84(9):3921-3928.
20. Cao L. *Carrier-Bound Immobilized Enzymes: Principles, Application and Design*. John Wiley & Sons; 2006.
21. M. Kisler J, Dähler A, W. Stevens G, J. O'Connor A. Separation of biological molecules using mesoporous molecular sieves. *Microporous Mesoporous Mater*. 2001;44:769-774.
22. Xiao F-S, Han Y, Yu Y, Meng X, Yang M, Wu S. Hydrothermally stable ordered mesoporous titanosilicates with highly active catalytic sites. *J Am Chem Soc*. 2002;124(6):888-889.
23. Zhu W, Wang J, Wu D, et al. Investigating the heavy metal adsorption of mesoporous silica materials prepared by microwave synthesis. *Nanoscale Res Lett*. 2017;12(1):323.
24. Bagheryan Z, Raoof J-B, Ojani R, Rezaei P. Development of a new biosensor based on functionalized SBA-15 modified screen-printed graphite electrode as a nano-reactor for Gquadruplex recognition. *Talanta*. 2014;119:24-33.
25. Huo S, Zhao H, Dong J, Xu J. Facile synthesis of ordered mesoporous zirconia for electrochemical enrichment and detection of organophosphorus pesticides. *Electroanalysis*. 2018;30(9):2121-2130.
26. Alberti S, Soler-Illia GJ, Azzaroni O. Gated supramolecular chemistry in hybrid mesoporous silica nanoarchitectures: controlled delivery and molecular transport in response to chemical, physical and biological stimuli. *Chem Commun*. 2015;51(28):6050-6075.
27. Pascual L, El Sayed S, Marcos MD, Martínez-Máñez R, Sancenón F. Acetylcholinesterase-capped mesoporous silica nanoparticles controlled by the presence of inhibitors. *Chem Asian J*. 2017;12(7):775-784.
28. Aznar E, Oroval M, Pascual L, Murguía JR, Martínez-Máñez R, Sancenón F. Gated materials for on-command release of guest molecules. *Chem Rev*. 2016;116(2):561-718.
29. Agostini A, Mondragón L, Coll C, et al. Dual enzyme-triggered controlled release on capped nanometric silica mesoporous supports. *ChemistryOpen*. 2012;1(1):17-20.
30. de la Torre C, Agostini A, Mondragón L, et al. Temperature-controlled release by changes in the secondary structure of peptides anchored onto mesoporous silica supports. *Chem Commun*. 2014;50(24):3184-3186.
31. de la Torre C, Mondragón L, Coll C, et al. Cathepsin-B induced controlled release from peptide-capped mesoporous silica nanoparticles. *Chemistry*. 2014;20(47):15309-15314.
32. Mondragón L, Mas N, Ferragud V, et al. Enzyme-responsive intracellular-controlled release using silica mesoporous nanoparticles capped with ε-poly-L-lysine. *Chemistry*. 2014;20(18):5271-5281.
33. Santos-Figueroa LE, Giménez C, Agostini A, et al. Selective and sensitive chromofluorogenic detection of the sulfite anion in water using hydrophobic hybrid organic–inorganic silica nanoparticles. *Angew Chem*. 2013;125(51):13957-13961.
34. Climent E, Gröninger D, Hecht M, et al. Selective, sensitive, and rapid analysis with lateral-flow assays based on antibody-gated dye-delivery systems: the example of triacetone triperoxide. *Chemistry*. 2013;19(13):4117-4122.
35. Salinas Y, Solano MV, Sørensen RE, et al. Chromo-fluorogenic detection of nitroaromatic explosives by using silica mesoporous supports gated with tetrathiafulvalene derivatives. *Chemistry*. 2014;20(3):855-866.
36. Sancenón F, Pascual L, Oroval M, Aznar E, Martínez-Máñez R. Gated silica mesoporous materials in sensing applications. *ChemistryOpen*. 2015;4(4):418-437.

37. Zhao D, Sun J, Li Q, Stucky GD. Morphological control of highly ordered mesoporous silica SBA-15. *Chem Mater*. 2000;12(2):275-279.
38. Yiu HHP, Wright PA, Botting NP. Enzyme immobilisation using SBA-15 mesoporous molecular sieves with functionalised surfaces. *J Mol Catal B: Enzymatic*. 2001;15(1-3):81-92.
39. Singh AK, Flounders AW, Volponi JV, Ashley CS, Wally K, Schoeniger JS. Development of sensors for direct detection of organophosphates. Part I: immobilization, characterization and stabilization of acetylcholinesterase and organophosphate hydrolase on silica supports. *Biosens Bioelectron*. 1999;14(8-9): 703-713.
40. Dinesh B, Shalini Devi KS, Kumar AS. Curcumin-quinone immobilised carbon black modified electrode prepared by in-situ electrochemical oxidation of curcumin-phytonutrient for mediated oxidation and flow injection analysis of sulfide. *J Electroanal Chem*. 2017;804:116-127.
41. Pundir CS, Chauhan N. Acetylcholinesterase inhibition-based biosensors for pesticide determination: a review. *Anal Biochem*. 2012;429(1):19-31.
42. Rui Y, Wu X, Ma B, Xu Y. Immobilization of acetylcholinesterase on functionalized SBA-15 mesoporous molecular sieve for detection of organophosphorus and carbamate pesticide. *Chin Chem Lett*. 2018;29(9):1387-1390.
43. Saleem M, Rafiq M, Seo S-Y, Lee KH. Acetylcholinesterase immobilization, characterization and comparison of porous silicon immobilized enzyme activity with the free counter part. *Biosci Rep*. 2016;36(2):e00311.
44. Nanda Kumar D, Alex SA, Chandrasekaran N, Mukherjee A. Acetylcholinesterase (AChE)-mediated immobilization of silver nanoparticles for the detection of organophosphorus pesticides. *RSC Adv*. 2016;6(69):64769-64777.
45. Ganesana M, Istarnboulie G, Marty J-L, Noguer T, Andreescu S. Site-specific immobilization of a (His) 6-tagged acetylcholinesterase on nickel nanoparticles for highly sensitive toxicity biosensors. *Biosens Bioelectron*. 2011;30(1):43-48.
46. Chauhan N, Pundir CS. An amperometric biosensor based on acetylcholinesterase immobilized onto iron oxide nanoparticles/multi-walled carbon nanotubes modified gold electrode for measurement of organophosphorus insecticides. *Anal Chim Acta*. 2011;701(1):66-74.
47. Kalhor MM, Rafati AA, Rafati L, Rafati AA. Synthesis, characterization and adsorption studies of amino functionalized silica nano hollow sphere as an efficient adsorbent for removal of imidacloprid pesticide. *J Mol Liq*. 2018;266:453-459.
48. Wagner T, Krotzky S, Weiß A, et al. A high temperature capacitive humidity sensor based on mesoporous silica. *Sensors*. 2011;11(3):3135-3144.
49. Upadhyay S, Rao GR, Sharma MK, Bhattacharya BK, Rao VK, Vijayaraghavan R. Immobilization of acetylcholineesterase–choline oxidase on a gold–platinum bimetallic nanoparticles modified glassy carbon electrode for the sensitive detection of organophosphate pesticides, carbamates and nerve agents. *Biosens Bioelectron*. 2009;25(4):832-838.

SUPPORTING INFORMATION

Additional supporting information may be found online in the Supporting Information section at the end of the article.

How to cite this article: Palanivelu J, Chidambaram R. Acetylcholinesterase with mesoporous silica: Covalent immobilization, physiochemical characterization, and its application in food for pesticide detection. *J Cell Biochem*. 2019;1-10.
https://doi.org/10.1002/jcb.28369